Invention Journal of Research Technology in Engineering & Management (IJRTEM)
ISSN: 2455-3689
www.Ijrtem. com Volume 3 Issue 6 ǁ September-October 2019 ǁ PP 06-15

Numerical Study of Flow Velocity in The Intake Manifold of Single Cylinder Port Operated Two-Stroke Spark Ignition Engine

[1,]Lawal Muhammed Nasir, [2,]Muhammed Nurudeen
[1]*Faculty of Engineering, University of Abuja, FCT, Abuja Nigeria*
nasir.lawal@uniabuja.edu.ng
[2]*National Inland Waterways Authority, Lokoja, Kogi State Nigeria*
Amdeen24@gmail.com

ABSTRACT: *Performance of internal combustion engine (ICE) is chiefly dependent on the supply rate and hence, in-flow velocitythrough the intake manifold. Fresh charge through the intake manifold experiences velocity gradient due togeometric constraints and fluid resistance [1]. The reduction in flow velocity causes incomplete delivery before the complete closure of intake port. This study uses unidirectional transient velocity model to determine time required for complete charge delivery into the crankcase/cylinder in two stroke spark ignition engines. Finite difference scheme is employed to approximate the model for unsteady non-uniform flow. A bench work involving measurements of the average flow rates at different intake pressures and engine speeds is conducted using a ported operated single cylinder two-stroke spark ignition C12-HS engine utilizing pre-mixed fuel. It is observed that at low engine speeds and intake pressures, flow is predominantly non-uniform requiring about1.5 to 6.5 ms for maximum delivery, while unsteady condition dominates the flow at higher speeds and manifold pressures with maximum delivery occurring at about 1.25 ms; which tends to agree reasonably with the intake manifold design of Singh for axial velocity against manifold axial position [2], as well as the result of Jasen et al. [3], on runner length against engine speed.*

KEYWORDS: *Fresh-charge, delivery, velocity gradient, and two-stroke*

I. INTRODUCTION

The performance of anICE is dependent on the rate of fresh charge supplied to the cylinder [4]. The flow rate is a function of velocity of flow, intake geometry and state properties of the fluid. The velocity component of the function varies along the length of the manifold due to pressure gradient.The intake port to the crankcase/cylinder has fixed opened-down period over a cycle, at any given engine speed. As engines operate over a range of speeds, the fresh charge required for combustion is aspirates through the intake manifold [5]. Delivering this charge to the combustion chamber efficiently, is to a large extent a function of the dynamic variables in the intake manifold, and a lot of the engine's performances and environmental effects are dependent on it [4, 5]. Thus, maximizing charge delivery to the cylinder before the closure of IP is a necessary consideration during intake system design. In reality,part of the supplied charge does not reach the cylinder at the close of the IP. In actual operation however, some charges are locked out at closure time partly due to flow gradient [3, 6].From geometric point of view, the capability of an intake system to elaborate a large mass flow depends on the tuned length of the intake manifold as well as the port size,form and location. While from operation stand point, the flow rate depends on engine speed [6]. Matching engine speed with geometry is necessary for high performance. This is usually achieved through wave dynamics established due to vacuum pumping.Several devices/solutions are also introduced to improve aspirated mass ranging from super-charging systems [4] to utilization of surge tanks [7].

In the manifold, the supply chargetravels considerable distance between the throttle system and combustion chamber leading to supply time lag and sometimes cycle overlap due to interference of flow dynamics [7]. This scenariocauses charge supply to lag behind instantaneous engine demand and consequently results to poor performance in terms of power and emission. Conventionally, the ratio of the actual mass of aspirated charge to the instantaneous engine mass demand is defined as volumetric efficiency (or delivery ratio in two-stroke engine). The delivery ratio depends on pulsating effect associated with the flow dynamics in the manifold and can be optimized by geometrical tuning of the manifold. In all cases, the engine output, in terms of power and delivered torque, is proportional to the charge delivered [8, 20]. In operation, the supply of air into the manifold is controlled by the throttle disc linked to the accelerator pedal or handle by some lever mechanisms. For maximum engine speed, the valve is completely opened; and closed when idle with a ported supply as shown in Figure 1 [9], to keep the vehicle or plant from stalling.

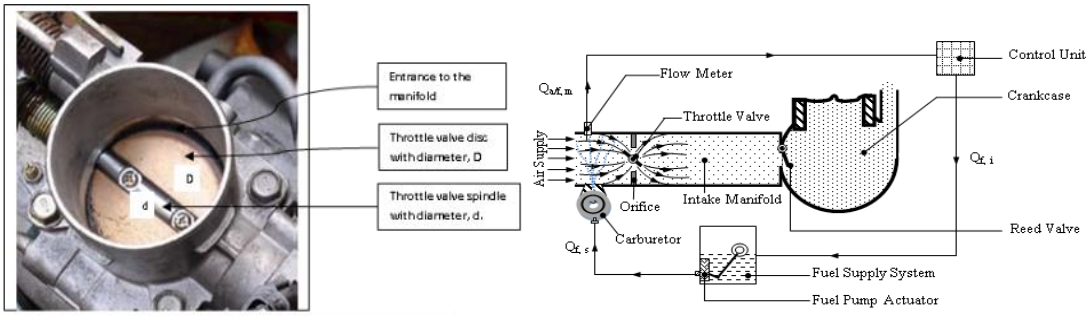

(a) Pictorial view of a throttle valve (b) Schematic diagram of an intake manifold

Figure 1: Elements of a throttle valve and intake Manifold system

Several numerical approaches have been used to analyze flow in the intake manifold ranging from one- to three-dimensional analyses. One dimensional *method of characteristics* to simulate flows in the intake manifold with the aim of understanding how the waves produced from running the engine affect its performance was studied using varying manifold length[2, 8, 9, 19, 17, 21]. A pulse wave method with adjustable valves to allow for individual variation in parameters and operation conditions was adopted in the length of the manifold. It was reported that pressure may be increased up to 5.4% by tripling the intake length and 2.3% by doubling it [9]. Laser Doppler Anemometry (LDA) apparatus has also been used to observe flow in the intake manifold of a motorized compression ignition engine at low speed range of 300 to 1100 rpm with the aid of plexi-glass windows placed at different positions in the manifold branches to obtain mean value of in-cylinder radial and axial velocity distribution [7]. The flow in each pipe was reported to be approximately uni-dimensional and possesses repeatable format across cycles with uniform but low turbulent during induction (that is when the IP is opened down) [10].

To improve stoichiometric air flow (an exact quantity of instantaneous mass flux into the cylinder), air mass sensor (AMS) and the speed density method (SDM) has been used to provide feedback to compensate for manifold loss and other system delays [8, 11]. The comparative study identifies AMS to be more efficient than its SDM, though the relative high cost and technical reliability has made the use SDM more prominent. The researchers reported that estimate of the flow rate through the throttle can be utilized to give lead information required for instant air-fuel ratio for fuel injection models – with little or no phase lag [8]. In summary, the flow rate in the intake manifold depends on both the pressure difference between any two regions, the supply cross-sectional area and the engine speed. The system is more or less functioning like a vacuum pump, utilizing the creation of vacuum pressure by the piston movement to drive the cycle. How much of the fresh charge that is delivered to the cylinder at the close of intake port, is a function of the flow dynamics. With the system geometry fixed in terms of control volume and flow area, flow velocity model can be used to identify the range of initial pressure that will yieldmaximum power and minimum emission of harmful gases, as well as the time required to deliver maximum quantity of fresh charge to the cylinder.This study first established the instantaneous piston speeds of some common two-stroke engines, during the IP open-down period based on their geometric data and assumed engine speeds. This is followed by determination of the mean effective time-area for each port aperture. Flow is then simulated numerically with assumed constant flow rates through the established mean area to identify fraction of time associated with the time-area scale that allows complete delivery. The result so obtained is compared with the open-down period directly obtained from the operation of the manifold via a motored process.

II. MATERIALS AND METHODS

Fundamentally, the flow rate of a fluid is a function of density, flow area and velocity. With the fluid properties and control volume geometry relatively fixed, velocity of flow becomes the main determinant of how much fresh charge is aspirated. The velocity of flow that is of interest in the manifold is that during the open down period of the intake port into the crankcase or the cylinder. In addition, the initial value of such velocity in important. To identify this initial value, this study uses unidirectional transient velocity model to determine optimum range of initial velocity based on manifold differential pressure, required to produce maximum charge delivery into the crankcase/cylinder in two stroke spark ignition engines. A mathematical model is developed based on nervier stoke equations for flow through the manifold of a two-stroke SIE. A 1-D finite difference scheme is utilized to solve the model. The equations were simulated with engine specifications of C12 – HS Two stroke SIE, initial and boundary conditions as inputs and validated using the same C12 – HS 2-stroke SIE.

III. MODEL FORMULATION

One-dimensional unsteady compressible flow momentum equation carved out of nervier stoke equation is used to model the flow velocity in the intake manifold. Geometrical variations in terms of cross-sectional area, tube entrants and bents are factored in. all other forces are assumed negligible[2, 12, 13, 18], since:

$$\frac{L}{D} > 5,\ \frac{\partial V_x}{dx} \gg \frac{\partial V_x}{dr},\quad \text{and} V_r \ll V_x$$

The flow can be represented with Nervier Stokes equation as [13]:

$$\frac{d\vec{V}}{dt} = \frac{1}{\rho}\nabla p + \frac{\mu}{\rho}\nabla^2\vec{V} + \frac{1}{3}\frac{\mu}{\rho}\nabla(div\ \vec{V}) \quad (1)$$

where the total differential, $\frac{d\vec{V}}{dt} = (\vec{V}\cdot\nabla)\vec{V}$

The corresponding simplifiedscalar form of Equation (1) along the intake manifold pipe is [13]:

$$V_x\frac{\partial V_x}{dx} + \frac{\partial V_x}{dt} = -\frac{1}{\rho}\frac{\partial p}{dx} + \frac{4}{3}\frac{\mu}{\rho}\left(\frac{\partial^2 V_x}{dx^2}\right) \quad (2)$$

For an infinitesimal elemental length Δx along the manifold axis, flow may be considered incompressible and theheadloss across Δxexpressed as $\Delta h = \frac{v^2}{2g}\left(\lambda\frac{\Delta x}{D} + \sum\zeta\right)$[14**]**, which can be expressed in terms of pressure drop as:

$$\Delta P = \frac{8\rho Q^2}{\pi^2 D^4}\left(\lambda\frac{\Delta x}{D} + \sum\zeta\right) \quad (3)$$

Dividing Equation (7) by Δx, and setting $\frac{\Delta P}{\Delta x} \to \frac{\partial P}{\partial x}$ as $\Delta x \to 0$, yields:

$$\frac{\partial P}{\partial x} = \frac{8\rho Q^2}{\pi^2 D^4}\left(\frac{\lambda}{D} + \frac{\sum\zeta}{\Delta x}\right) \quad (4)$$

Equation (4) is substituted in Equation (2) with further arrangement and simplification by expressing$Q = AV$, to give:

$$\frac{\partial V_x}{\partial t} - \mu\left(\frac{1}{\rho} + \frac{1}{3}\right)\frac{\partial^2 V_x}{\partial x^2} + V_x\frac{\partial V_x}{\partial x} + \frac{{V_x}^2}{2}\left(\frac{\lambda}{D} + \frac{\sum\zeta}{\Delta x}\right) = 0 \quad (5)$$

Numerical Analysis

Finite difference scheme is used for discretization as follows:

i. Time discretization - 1st order forward difference
ii. Pressure discretization -1st order central difference
iii. 1st order spatial derivative - 1st order backward difference
iv. 2nd order spatial derivative - 2nd order central difference

From Equation (5), the following parameters were defined.$C_1 = \mu\left(\frac{1}{\rho} + \frac{1}{3}\right)$, $C_2 = V_x{}_i^j$, and $C_3 = \frac{1}{2}\left(\frac{\lambda}{D} + \frac{\sum\zeta}{\Delta x}\right)$

$$\frac{\partial V_x}{\partial t} = C_1\frac{\partial^2 V_x}{\partial x^2} - C_2\frac{\partial V_x}{\partial x} - C_3\frac{{V_x}^2}{2} \quad (6)$$

Equation (5) can be approximated using the assumed schemes as:

$$\frac{V_x{}_i^{j+1} - V_x{}_i^j}{\Delta t} = C_1\left[\frac{V_x{}_{i+1}^j - 2V_x{}_i^j + V_x{}_{i-1}^j}{\Delta x^2}\right] - C_2\left[\frac{V_x{}_i^j - V_x{}_{i-1}^j}{\Delta x}\right] - C_3\left[V_x{}_i^j\right]^2 \quad (7)$$

And for the pressure drop in Equation (4) in terms of flow velocity is:

$$\frac{P_x{}_{i+1}^j - P_x{}_{i-1}^j}{2\Delta x} = \frac{\rho\left[V_x{}_i^j\right]^2}{2}\left(\frac{\lambda}{D} + \frac{\sum\zeta}{\Delta x}\right) \quad (8)$$

Where $V_x{}_i^j$ is the flow velocity at any given position *i* and corresponding time *j* in x-direction.

$$\left[V_x{}_i^j\right]^2 = 2c_pT_o\left[1 - \left(\frac{P_{xi}}{P_o}\right)^{\frac{\gamma-1}{\gamma}}\right] \quad (9)$$

Thus, the instantaneous value of pressure at any position and time is

$$P_x{}_{i+1}^j = P_x{}_{i-1}^j + C_3\rho c_pT_o\Delta x\left[1 - \left(\frac{P_{xi}}{P_o}\right)^{\frac{\gamma-1}{\gamma}}\right] \quad (10)$$

Error magnitude and Correction Factor: From Taylor's series the instantaneous change in velocity may be expressed as:

$$\frac{V_x{}_i^{j+1} - V_x{}_i^j}{\Delta t} = \left(\frac{\partial V_x}{\partial t}\right) + \frac{\Delta t}{2!}\frac{\partial}{\partial t}\left(\frac{\partial V_x}{\partial t}\right) + \frac{\Delta t^2}{3!}\frac{\partial^2}{\partial t^2}\left(\frac{\partial V_x}{\partial t}\right) + \cdots \quad (11)$$

Substituting for$\left(\frac{\partial V_x}{\partial t}\right)$, in Equation (11) using Equation (6) will produce:

$\frac{V_{x_i}^{j+1}-V_{x_i}^{j}}{\Delta t}=\left(C_1\frac{\partial^2 V_x}{\partial x^2}-C_2\frac{\partial V_x}{\partial x}-C_3\frac{V_x{}^2}{2}\right)+\frac{\Delta t}{2!}\frac{\partial}{\partial t}\left(\boldsymbol{C_1\frac{\partial^2 V_x}{\partial x^2}-C_2\frac{\partial V_x}{\partial x}-C_3\frac{V_x{}^2}{2}}\right)+\frac{\Delta t^2}{3!}\frac{\partial^2}{\partial t^2}\left(C_1\frac{\partial^2 V_x}{\partial x^2}-C_2\frac{\partial V_x}{\partial x}-C_3\frac{V_x{}^2}{2}\right)+\cdots$ (12)

The effect of approximation to Numerical dispersion in time is limited to second term highlighted in Equation (12). Thus,

$\frac{\partial}{\partial t}\left(C_1\frac{\partial^2 V_x}{\partial x^2}-C_2\frac{\partial V_x}{\partial x}-C_3\frac{V_x{}^2}{2}\right)=-C_3\left(V_{x_i}^{j}\right)^2-C_2\frac{V_{x_i}^{j}-V_{x_{i-1}}^{j}}{\Delta x}+\left[C_1-\frac{\Delta t}{2}C_2{}^2-C_2\frac{\Delta t}{2}\right]\frac{V_{x_{i+1}}^{j}-2V_{x_i}^{j}+V_{x_{i-1}}^{j}}{\Delta x^2}$ (13)

Thus, the overall correction factor interms of the established parameters is:

$C^*=C_1-\frac{\Delta t}{2}(C_2+C_2{}^2)$ (14)

Stability Criteria : For stability, the attributed error$\boldsymbol{\epsilon}$, remains bounded as it increases from its previous value at j to its current value at j+1, [13, 15]. For this condition to hold, the modulus of the eigenvalues of coefficients of the required velocities at chosen points $x_1, x_2, \ldots, x_n$,as a vector $\boldsymbol{A}(n\times n)$, must be bounded as:

$|\varsigma|\le 1,\quad for\ k=1,2,3,\ldots,n;$ (16)

Where $\boldsymbol{A}$ is the matrix of the coefficients of the required velocities, ς, is the eigenvalues of $\boldsymbol{A}$.

The Greschgorin's circle theorem [16], is used to determine the eigenvalues of the matrix A as:

$\left|\varsigma-\boldsymbol{A}_{s,s}\right|=\lambda_s$ (17)

Where λ_s is the sum of all individual modulus of the elements on the s-row, and $\boldsymbol{A}_{s\text{-}s}$ are the elements on the diagonal.

Equation (13) is further resolved by multiplying through by$(\Delta t\cdot\Delta x^2)$, and simplified to give:

$V_{x_i}^{j+1}=(K_1+K_2)V_{x_{i-1}}^{j}+(1-2K_1-K_2-K_3)V_{x_i}^{j}+K_1V_{x_{i+1}}^{j}$ (18)

Where: $K_1=(\Delta t\cdot C_1);\quad K_2=(\Delta t\cdot\Delta x\cdot C_2);\quad K_3=(\Delta t\cdot\Delta x^2\cdot C_3\cdot V_{x_i}^{j}),$

Further parametric grouping gives:

$V_{x_i}^{j+1}=G_1V_{x_{i-1}}^{j}+G_2V_{x_i}^{j}+G_3V_{x_{i+1}}^{j}$ (19)

Where: $G_1=(K_1+K_2);\ G_2=(1-2K_1-K_2-K_3);and\ G_3=K_1$

Applying the Greschgorin's circle theorem to matrix A, above will give $\left|\varsigma-A_{s,s}\right|=\lambda_s$. That is:

$|\varsigma-G_2|\le G_1+G_3$ (21)

Removing the absolute sign and simplifying using backward substitution of the chains of parameters, gives:

$1-4K_1-2K_2-K_3\le\varsigma\le 1-K_3$ (22)

For stability, $-1\le\varsigma\le 1$. Thus, fromthe right hand side of Equation (22),K_3 must be positive, forςto be less than 1, while on the left hand side, $\varsigma\ge -1$ only when $1-4K_1-2K_2-K_3\ge -1$ from which the stability equation is obtained as:

$4K_1+2K_2+K_3\le 2$ (22)

Further backward substitution in terms of initial starting parameters: $C_1,\ C_2\ and\ C_3$, gives the required time step limit for stability as:

$\Delta t\le\frac{2}{\left(4C_1+2\Delta x\cdot C_2+\Delta x^2\cdot C_3\cdot V_{x_i}^{j}\right)}=\frac{2}{4\mu\left(\frac{1}{\rho}+\frac{1}{3}\right)+\left[2\Delta x+\Delta x^2\cdot\frac{1}{2}\left(\frac{\lambda}{D}+\frac{\sum\zeta}{\Delta x}\right)\right]V_{x_i}^{j}}$ (23)

whereΔt is the maximum time step that allows convergence.

Matrix Representation of the model variables : In matrix form, the model variables of equation (19) can be represented as:

$$\begin{bmatrix}V_{x_1}\\V_{x_2}\\V_{x_3}\\\vdots\\V_{x_n}\\V_{x_{n+1}}\end{bmatrix}^{j+1}=\begin{bmatrix}1 & & & \cdots & & \\ G_1 & G_2 & G_3 & \cdots & & \\ & G_1 & G_2 & \cdots & G_3 & \\ \vdots & \vdots & \vdots & \cdots & \vdots & \vdots\\ & & G_1 & \cdots & G_2 & G_3\\ & & & \cdots & G_1 & G_2\end{bmatrix}\times\begin{bmatrix}V_{x_1}\\V_{x_2}\\V_{x_3}\\\vdots\\V_{x_n}\\V_{x_{n+1}}\end{bmatrix}^{j}$$ (20)

Initial and boundary conditions

Inlet velocity is take to be 0 m/s,

Experimental Setup:A C12-HS intake manifold model of diameter 21.3 mm and approximate equivalent straight length 204 mm coupled with a single-cylinder 56 cc spark ignition engine operating on two-stroke cycle with a rated power of 3.5 HP and a maximum speed of 7,600 RPM is used. The engine is equipped with two ports –

intake and exhaust into and out of the cylinder respectively. For maximum engine performance, the quantity of air supply through the manifold per unit time is maximized. In this work, the manifold dynamic performances were observed. The characteristics of air passing through the intake manifold into the combustion chamber is measured with the aid of a tuned pipe of length 206 mm. Part of the experimental results obtained that falls at least, 5 cm away from both edges were used to conduct numerical simulation of flow through the manifold, using the vacuum differential pressure model across the intake control volume/length. The test bench consisted of a motored engine that uses only air as the working fluid with the piston and cylinder acting as suction pump downstream of the manifold. The pressure of flow in the intake manifold is varied by altering the RPM of variable motor that drives the engine. The air supply is controlled by the adjustable throttle plate set to match the speed of the variable motor. Figure 2, shows the schematic representation of the arrangement in which the original intake manifold length (a), is replaced with an equivalent straight length pipe (b). Four (4) holes of diameter 8 mm each are drilled along the length of the equivalent pipe with 40 mm intervals. Only a hole is left open with pizometric pressure sensor installed to estimate the differential vacuum pressure at each position while running on differentoperating conditions of throttle valve and engine motor speed.

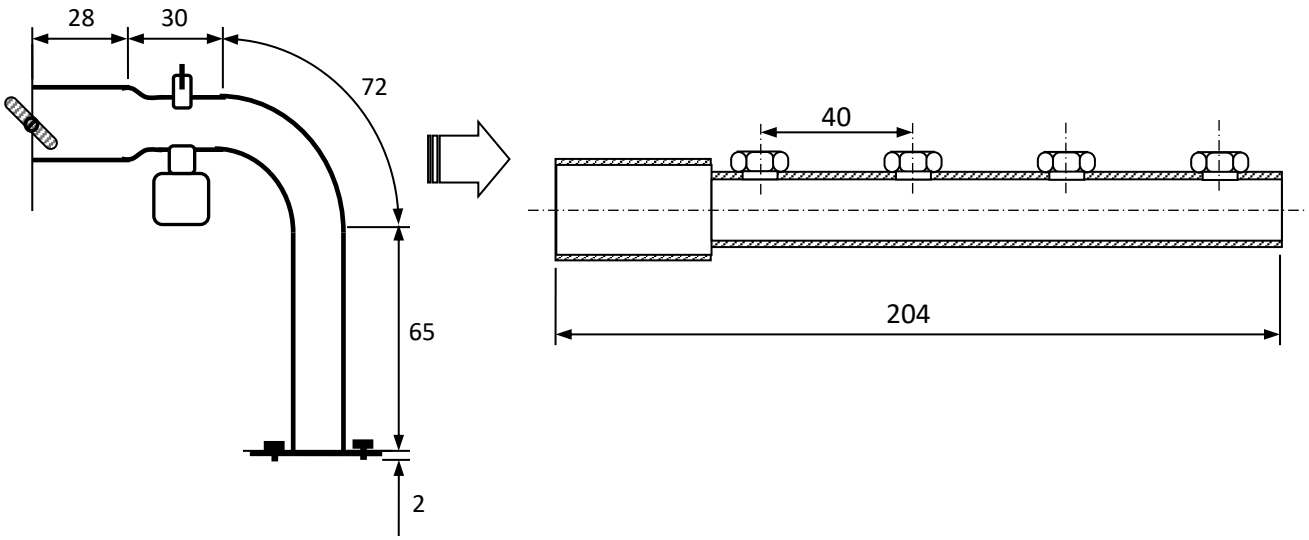

Figure 2: Schematic diagram of the intake manifold and its equivalent Length

Figure 3: C12 – HS Two stroke spark ignition engine
Source: NITT Two stroke Auto Lab Unit Zaria

A 5 digitalLCD tachometer with an output accuracy of 0.05% + 1dp and a resolution of 1 rpm (over a range of 0.5 to 10,000 rpm) is used to measure the revolution per minute of the variable speed electric motor. The maximum rpm measured is displayed with the average value side by side. A data acquisition unit is attached to keep logs of at different pressure and speed readings.The length of the intake pipe is divided into four parts, leaving outabout 5 cm from each end. Holes of 8 mm diameter are drilled at the four equidistance marked points, and an 8 mm nut

is weldedon each to flush with the holes for holding the pressure measuring device in place.The engine is motor driven, and the air supply is naturally aspirated. At different engine speeds, the manifold pressure/velocity is sensed and measured by the piezometer and corresponding signals passed to the VDAS. At the VIDAS, the data is statistically analyzed to give average pressure values per cycle, while all other holes were sealed with M8 bolts. To minimize leakages, thread tape was wrapped two to three turns to seal thread irregular contours.

IV. RESULTS AND ANALYSIS

Velocity Gradient along the axial Length of Manifold Pipe : Figure 4.1 presentsthe variation of velocitywith time in the manifold at points 0 mm, 20 mm, 40 mm and 60 mm marks along the length of the manifold. The point zero is taken to be at the throttle plate. The engine speed is 1000 rpm and the throttle is 45º. Velocity is simulated for an initial manifold pressures $P_m(t_o)$ of0kPa corresponding to a minimum vacuum pressure of 101.3 kPa.

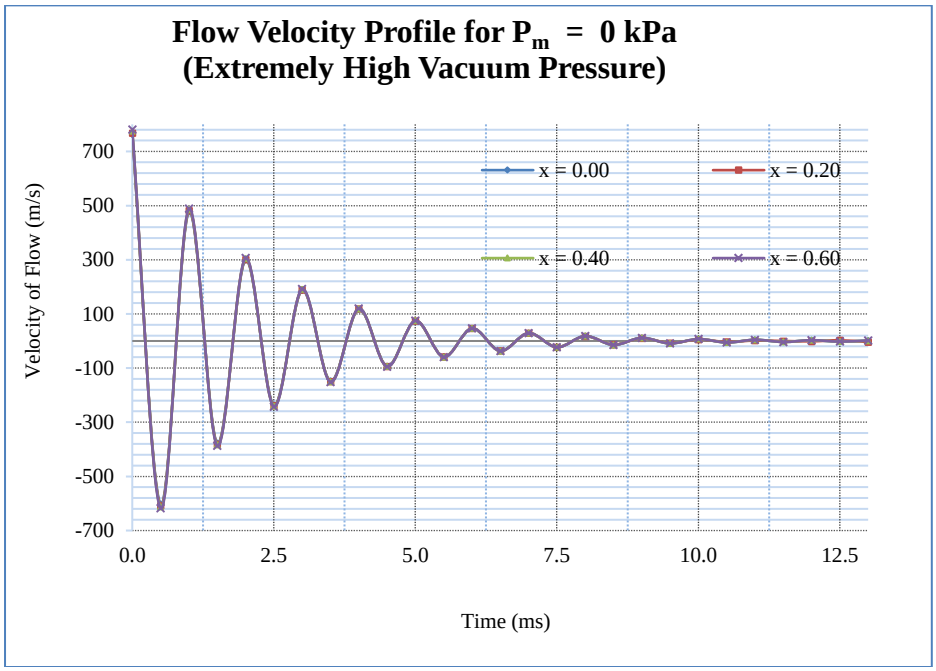

Figure 4.1: Variation of velocity of flow over opened down period of intake ports at an initial differential pressure of 10 kPa in the manifold

From Figure 4.1, at an initial manifold pressure,$P_m(t_o)$ = 0 kPa, engine speed of 1000 rpm and a throttle angle of 45º, the velocity of flow is extremely high and oscillates periodically with its consecutive amplitudes decaying exponentially to zero (where the flow seizes). The time take by the resultant flow to completely stop is about 7.5 ms (milliseconds). At an engine speed of 1000 rpm, the cycle period in two-stroke engine is 60 ms (or 30 ms per stroke). For an intake port (IPO = 50ºbTDC and IPC = 50ºaTDC) the open-down period is 100º. Thus, the period t_p in seconds as given by Gordon (1973), is t_p = 100º/(1000 rpm * 6) = 16.7 ms.Thus, at extremely low initial manifold pressure, there is abundant time for the incoming charge to enter the crankcase or cylinder (as the case may be) before the closure of the intake port. This is evident from the fact that the time required to stop flow (7.5 ms) is approximately half of the time the intake port is opened down (16.7 ms). Also, the flow velocity is very high and unsteady as its instantaneous value varies from time to time; but, uniform along the length of the manifold since the graphs of velocities at points x = 0, 20, 40, and 60 mm when t = 0 ms are not separated. Both conditions support high natural aspiration and delivery fresh charges to the crankcase. However, the power produced is extremely low as the resultant flow velocity in figure 4.2 depicts. The blue graph is for the simulated values while the one in red is for experimental values.

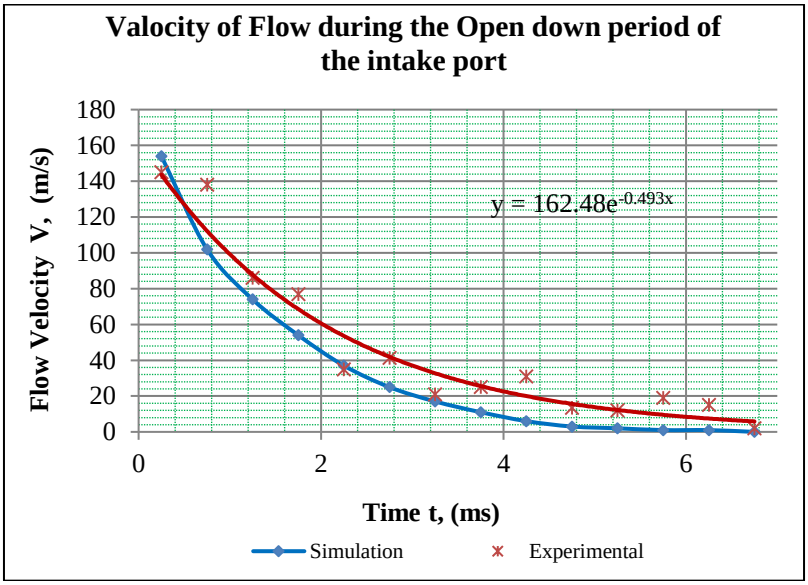

Figure 4.2: Resultant simulated and experimental velocity of flow over time in intake manifold

The resultant flow velocity in Figure 4.2 has a maximum value slightly above 160 m/s and decays over 5.25 ms to zero. The limited power output is due to the oscillatory reversal of flow established by pressure wave propagation as much of the aspirated charges were eventually lost. Figure 4.3 presents the variation of velocity flow with timeat aninitial manifold pressures P_m (t_o) is 10 kPa. Thus, the minimum vacuum pressure is 92.5 kPa (101.325 kPa – 10 kPa), at an engine speed of 4,000 rpm and throttle angle of 60º.

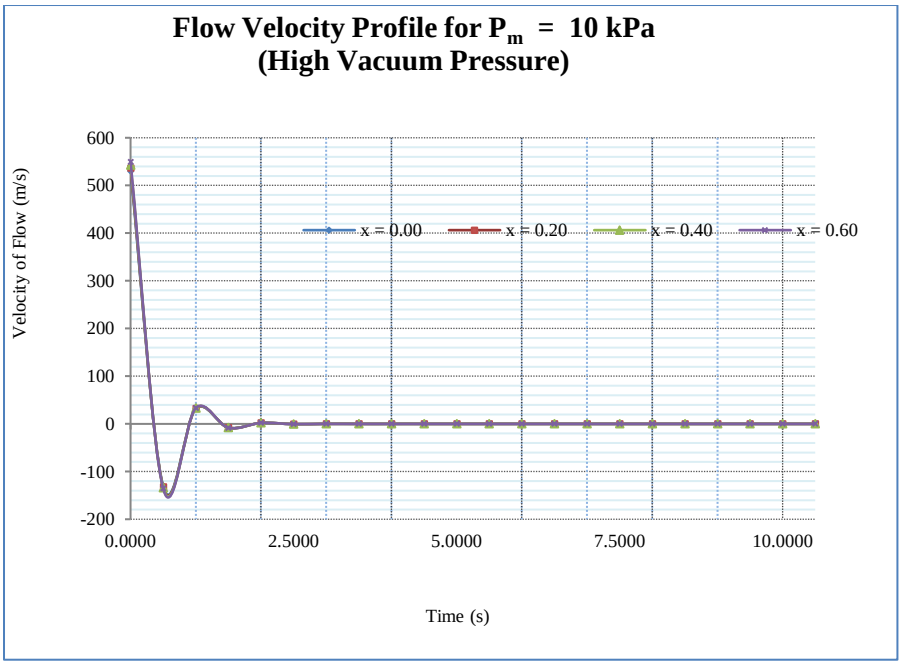

Figure 4.3: variation of velocity of flow over opened down period
of intake ports for an initial differential pressure of 10 kPa in the manifold

From Figure 4.3, at an initial manifold pressure, P_m (t_o) = 10 kPa, the velocity of flow is still high and oscillates for a short while and finally reduces abruptly to zero. At 4,000 rpm and a throttle angle of 60º, the time taken by the resultant flow to completely stop is about 2.5 ms (milliseconds). The engine cycle period is20 ms (or 10 ms per stroke) and the open-down duration of the intake port is3.4 ms. There is still enough time for the incoming

charge to arrive the crankcase or cylinder before the intake port closes. The flow velocity is still high and remains unsteady. The velocities at x = 0, 20, 40, and 60 mm is the same everywhere and hence uniform as the graphs are non-separated. The power produced is high and much of the supply charge is delivered.Figure 4.3 presents velocity flow variation with time in the manifold at points 0 mm, 20 mm, 40 mm and 60 mm marks along the length of the manifold. The engine speed is 7,000 rpm (max) and the throttle is 75° and the initial differential pressures P_m (t_o) = 100 kPa.

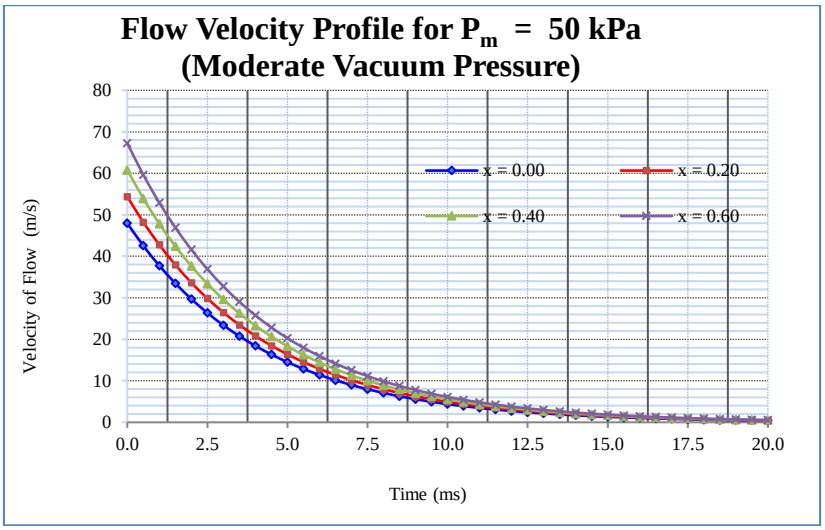

Figure 4.3: variation of velocity of flow over opened down period
of intake ports for an initial differential pressure of 10 kPa in the manifold

From Figure 4.3, the initial differential pressure is 100 kPa, the mean velocity of flow is now low and acoustic effect of oscillation, phased out. Immediately the port is opened down, there is slight variation in velocity of flow between points x = 0, 20, 40 and 60 mm marks a long the manifold. This leads to the separation of the velocity graphs showing beginning of non-uniformity of flow in the manifold. They all reduceexponentially to zero after about 20 ms. At an engine speed of 7,000 rpm and a throttle angle of 75° the time taken by the resultant flow to completely stop is about 20 ms (milliseconds). The engine revolution period is 8.6 ms (or 4.3 ms per stroke) and the open-down duration of the intake port is approximately 1.5 ms.If variation in density of supply charge and flow area are considered negligible, then, lots of the charge will not be delivered to the crankcase or cylinder as the velocity of flow is considerably inadequate to deliver it before the port closes.Figure 4.4 presents velocity flow variation with time in the manifold at positions 0, 20, 40 and 60 mm marks along the length of the manifold. The engine speed remains at 7,000 rpm (max) and the throttle angle is 75°, but the initial differential pressures P_m (t_o) is slightly less than atmospheric value.

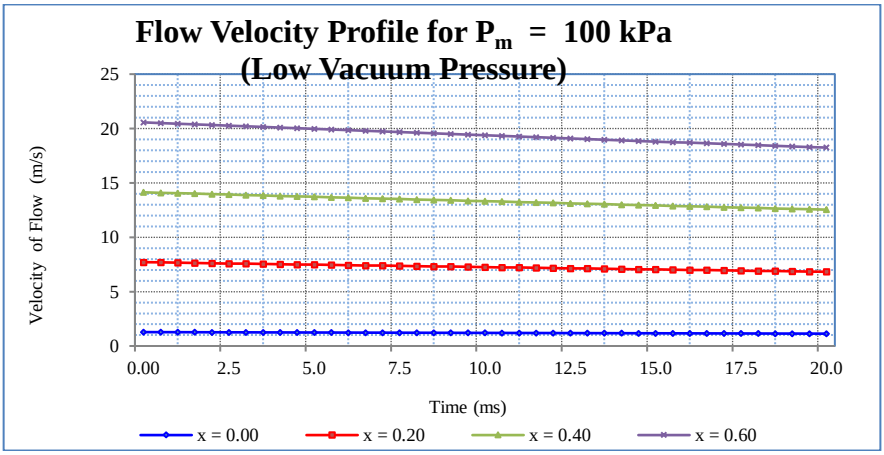

Figure 4.4: variation of velocity of flow over opened down period
of intake ports for an initial differential pressure of 10 kPa in the manifold

From the graph of Figure 4.3, the initial differential pressure is 10140 kPa, the mean velocity of flow is now extremely low with a maximum value of about 21 m/s. There is wide separation in velocity of flow at different locations of x (0, 20, 40 and 60 mm). The average difference is about 6.5 m/s. This indicates that flow becomes absolutely non-uniform. In addition, the graphs become flattened as the differential pressure approaches atmospheric value; showing that at all times the velocity is approximately the same. Thus, it can be concluded that the flow at this stage is steady but non-uniform. At 7,000 rpm and 18 mm port height, the open-down duration is 1.5 ms while the flow velocity approaches zero at infinity. Thus, most of the supply charge will be blocked out without getting to the crankcase/cylinder.

V. CONCLUSION

A mathematical model, based on the Nervier Stokes compressible flow conservation equations, was developed to predict the dynamic behaviors of fresh charge supply into the intake manifold of two-stroke spark ignition engine and its impact on the quantity of supply delivered to the cylinder/crankcase while intake is opened down. Haven established the thermofluid and geometric flow constraints, stability criteria, initial and boundary conditions were identified, the modeled equation was solved explicitly using finite difference approach. Simulation of the model equation for elemental locations of 0.05 mm along the manifold axis and time steps of 0.001s were applied to study the peculiar dynamic behaviors of the intake manifold used to validate the model. In order to observe the effects of dynamics of flow on supply quantity, the manifold vacuum pressures were varied and kept relatively constant; while variation in flow velocity were observed in four different locations along the axis. For highvacuum pressure of about < or = – 100 kPa, flow is found to be uniform, unsteady and decays exponentially. On the other hand, at low vacuum pressure, flow is steady and non-uniform. At moderate vacuum pressure,the flow becomes non-uniform and non-steady; which is most effective for maximum flow into the engine. The optimum vacuum pressure range is between 57 kPa (when the flow begins to lose its uniformity) and 88.5 kPa (where the gradient of the curves is $\leq$.0.05 m/s^2. Thus, keeping the vacuum pressure (and hence, supply dynamics) within a moderate range, the quantity of fresh charge delivery to the engine will be more effective during the open-down period of the intake port.

REFERENCES

[1] O. H. Ghazal, I. H. Qasem, M. Riyad, H. Abdelkader. "Modelling the effect of inlet manifold pipes bending angle on SI engine performance", *World Academy of Science, Engineering and Technology International Journal of Mechanical and Mechatronics Engineering*, Vol:6, No:9, 2012, pp. 1835 – 1838

[2] A. P. Singh (2014). "Intake Manifold Design Using Computational Fluid Dynamics". [Online]. Available: https://www.researchgate.net/publication/304112290 DOI: 10.13140/RG.2.1.3801.0483

[3] S. Jensen, N. S. Prasad, and K. Annamalai. "Effect of Variable Length Intake Manifold on a Turbocharged Multi-Cylinder Diesel Engine". Society of Automotive Engineers, Technical Papers, 2013. DOI: 10.4271/2013-01-2756. https://www.researchgate.net/publication/287040569

[4] S. A. Sulaiman, S. H. M. Murad, I. Ibrahim and Z. A. Abdul Karim. "Study of Flow in Air-Intake System for A Single-Cylinder Go-Kart Engine," *International Journal of Automotive and Mechanical Engineering (IJAME), Universiti Malaysia Pahang*, vol. 1, Pp. 91-104. 2010.

[5] I .Kazuei. (2003). *Effect of variable intake manifold on engine performance*. Subaru Automobile Company Quarterly Drive Magazine, New York, USA. Winter, 2003. [Online]. Available: http://www.drive.subaru.com/Win03

[6] J. Gordon. Two-Stroke Tuner's Handbook. *American Motorcyclist association. USA.* pp.75 – 89. 1973. [Online]. Available: https://www.bookdepository.com/Two-stroke-Turners-Handbook-Gordon-Jennings/9780912656410

[7] D. Bortoluzzi. "Fluid dynamic study of intake manifolds of internal combustion engines in presence of acoustic resonators". *Bright Hub Engineering*. Jun. 2014. [Online], Available: https://www.planetsoarer.com/resonator/ResonatorsAcoustic.htmm

[8] A. S. Green, and T. Moumtzis, (2002). "Use of inlet manifold design techniques for improving output of combustion engines". *Journal of Applied Thermal Engineering*. Vol. 22 (2002) 1519-1527, 2002.

[9] M. N. Lawal, "*Numerical and Experimental Study of Scavenging Process in two-stroke spark ignition engine that utilize premix fuel blend*", Ph.D Thesis, Dept. Mech. Eng., Federal University of Technology, Minna, Nigeria. 2015.

[10] B. M. Krishna and J. M. "Mallikarjuna. Characterization of flow through the intake valve of a single cylinder engine using particle image velocimetry", *Journal of Applied Fluid Mechanics*, Vol. 3, No. 2, pp. 23-32, 2010.

[11] G . Martin, and N. Apostolescu. "Calculation of gas velocity inside the cylinder of spark ignition engines," U.P.B. Sci. Bull., Series D, Vol. 68, No. 2, 59 – 76, 2006.

[12] H. L. John IV and H. L. John V. *A heat transfer text book*, 3rd ed, Massachusetts, Phlogiston press Cambridge (2006), pp. 281.

[13] S. Schneiderbauer and M. Krieger. "What do the Nervier Equations mean?" *European Journal of Physics*, 2013. [Online], Available: https://iopscience.iop.org/article/10.1007/BF01206939

[14] M. W. Frank *Fluid Mechanics*, 6th ed, London UK, McGra-Hill, (2003)..pp 383.

[15] H. Guang-Da and Z. Qiao (2010). "Bounds of Modulus of Eigenvalues based on Stein equation". *Kybernetika*, Volume 46, No. 4, 655 – 664. [Online], Available: http://dml.cz/dmlcz/140776

[16] M. Joneidi, H. B. Golestani and M. Ghanbari. "Eigen-gap of structure Transition Matrix: A new criterion for Image Quality assessment". *IEEE Conference Paper on Signal Processing and Signal Processing Education Workshop*, Uta, USA. Aug. 2015, [Online]. Available: http://ieeexplore.ieee.org/document/7369582?reload=true&arnumber=7369582
DOI: 10.1109/DSP-SPE.2015.7369582

[17] H. H. Al-Kayiem, H. A. AbdulWahhab and A. R. A. Aizz. "Computational analysis of flow characteristics in inlet and exhaust manifolds of single cylinder SIE", *Asian Journal of applied sciences*, Volume 10 (3): pp 102 – 115, 2017, Doi: 10.3923/ajaps.2017.102.115. [Online]. Available: https://scialart.net/abstract/?doi=ajaps.2017.102.115

[18] A. Valli and W. M. Zajaczkowski 1986. "Nervier Stokes Equation for Compressible Fluids: Global Existence and Qualitative Properties of the solutions in the General case". Journal of Communications in mathematical Physics, Vol. 103, Issue 2, pp. 259 – 296. [Online]. Available: https://link.springer.com/article/10.1007/BF01206939

[19] S. C. Kale and V. Ganesan. "A Study of Steady Flow through a SI Engine Intake system using CFD", *Journal of the Institute of Engineering I -MC*, Vol.86, 2005.

[20] K. V. Mukesh, V. Devvrat and S. Annand. "Design & Optimization of Intake Manifold of Carburettor Using Computational Fluid Dynamics". *International Journal of Engineering and Advanced Research Technology (IJEART) ISSN: 2454-929"0,* Vol. 3, (7), pp. 36 – 38. 2017.